

## Experimental and Theoretical Investigation for Performance of Shaft Journal Bearing Lubrication

Nader. Nasr<sup>1</sup>, \* Ahmed. Abdelsalam<sup>2</sup>, Amman. A. Ali<sup>3</sup> and Nour. A. Marey,\*<sup>4</sup>

<sup>1</sup>Department of Mechanical Engineering, College of Engineering and Technology, Arab Academy for Science, Technology and Maritime Transport, Alexandria, Egypt,

<sup>2</sup>Assistant Professor at the College of Engineering and Technology, Department of Mechanical Engineering, Arab Academy for Science, Technology and Maritime Transport, Alexandria, Egypt,

<sup>3</sup>Professor at the Institute of Maritime Upgrading Studies, Arab Academy for Science, Technology and Maritime Transport, Alexandria, Egypt,

<sup>4</sup>Second lecture, Institute of Maritime Upgrading Studies, Arab Academy for Science, Technology and Maritime Transport, Alexandria, Egypt, email: [nour\\_marine@aast.edu](mailto:nour_marine@aast.edu)

\*Corresponding author, DOI 10.21608/PSERJ.2023.242585.1269

Received 14-10- 2023,

Revised 4-11- 2023,

Accepted 12-11- 2023

© 2023 by Author(s) and PSERJ.

This is an open access article licensed under the terms of the Creative Commons Attribution International License (CC BY 4.0).

<http://creativecommons.org/licenses/by/4.0/>



### ABSTRACT

Hydrodynamic lubrication is definitely one of the foremost factors upon which the load carrying capacity within journal bearing mainly rely. Therefore, maintaining journal bearing lubrication away from boundary and transient lubrication regions is so instrumental in avoiding journal bearing wear. Accordingly, Universal Journal Bearing Test Rig (UJBTR) was specifically used for conducting wide range tests related to the versatile operational parameters utilizing different oil grades. Those were examined at the variable shaft speeds from 300 rpm up to 600 rpm, under the different applied loads from 50  $kg_f$  up to 510  $kg_f$ . The derived results were verified theoretically, where the error percentage hasn't exceeded 5.9 %. In light of the conducted study, oil film pressure was assured to rise with the increase of oil viscosity, loads, and speeds. For more detailed discussion, a dimensionless analysis was carried out to identify the impact percentage for viscosity, speed, and load on the hydrodynamic lubrication. It is observed that increasing load by 60 % had a considerable impact regarding the coefficient of friction where it reduced by 89 %. However, it turned out to have very negative impacts on hydrodynamic lubrication, where the hydrodynamic lubrication has moved into the hazardous boundary lubrication region. Based on the derived outcomes, operational factors are crucial impacts that shape journal bearing behavior considerably in real operating conditions either positively or negatively. Consequently, much consideration must be given to the selection of such factors so as to maintain and possibly enhance journal bearing performance.

**Keywords:** Journal Bearing Friction, Hydrodynamic Lubrication, Journal Bearing Operational Factors.

## 1. INTRODUCTION

Enhancing the operational condition of journal bearing systems is a top priority and a major concern for all those involved in the machinery industry throughout ages. Reducing operational and maintenance costs and extending the life time of the different equipment are but just a few of the numerous beneficial advantages that could be realized by working on the target. Also, considering the crucial function of the oil film lubrication in preventing the metal-to-metal contact regarding journal bearing, it is of topmost importance to thoroughly investigate and identify the most

critical operational factors affecting its performance in real operating conditions. Among the most instrumental operational factors contributing to the efficient behavior of such lubricating oil film, speed range, applied load and oil viscosity would come to the fore. In the research at hand, the effect of changing operating parameters involving shaft speed, oil viscosity as well as applied loads on journal shaft in regard to hydrodynamic lubrication is extensively investigated.

Several research endeavors have sought to achieve such enhancement via theoretical and experimental means alike. Binu et al. [1], Joy and Roy [2], Chatterton et al [3], Zhang et al [4] and Roy and Dey [5], introduced a

comprehensive analysis focused on the two axial groove journal bearing performance. Binu et al. [1], utilized a newly developed test rig under variable loads. They have examined the behavior of hydrodynamic pressure distribution at a speed range of 18 rps. The experimentally recorded pressures were noticed to be lower by roughly ~20 %, than those obtained theoretically. Joy and Roy [2], developed a computer program for optimizing the groove location and for calculating the steady-state hydrodynamic characteristics. The two-axial groove journal bearing design parameters showed good response if both grooves were positioned above the Z-axis. Also, flow rate was concluded to be a crucial parameter in journal bearing design. Furthermore, Chatterton et al. [3], examined several parameters under severe operating conditions with two axial grooves, the results were introduced and investigated under speed limits ranging from 66 rpm and up to 1440 rpm and loads of 0 kN and up to 350 kN. The pressure in the loaded part of the bearing were found to increase with the increase of the applied static load. Zhang et al. [4], discussed the potential of reducing computational costs via devising calculations concerning the fluid film force of a finitely long journal bearing with two axial grooves, pressure distribution was obtained based on Sommerfeld transformation. In addition, Roy and Dey [5], presented the uncertain hydrodynamic analysis of a two-axial groove journal bearing involving randomness in bearing oil viscosity and supply pressure. The study assured the importance of considering uncertainties of oil viscosity and supply pressure in design procedures. Marey et al. carried out a continuous bulk of research efforts combining both experimental and numerical means related to hydrodynamic journal bearing. Marey et al. [6] designed and constructed of a journal bearing test rig (JBTR). The established structure has made it possible to conduct thorough investigations into oil film pressure distribution at variable speeds and constant load. Marey [7] addressed the oil film pressure profile within journal bearing utilizing variable oil grades and applying speed variations from 50 rpm up to 400 rpm at constant load. Marey et al. [8] implemented major modifications on the journal bearing test rig which enlarged the potentials of the discipline and allowed for much more extensive experimental tests regarding the most critical operational factors affecting journal bearing. Marey and Ali. [9] designed and set up a novel measurement and control system for the Universal Journal Bearing Test Rig (UJBTR) constructed previously. Provided by full monitoring capabilities via Supervisory Control and Data Acquisition (SCADA) system, the structure has become fully controlled ensuring the accuracy of the obtained results. Additionally, Marey et al. [10] have implemented a comprehensive uncertainty and validation analysis for ascertaining the validity of the derived outcomes. Further, seeking to discern the full impacts of oil supply pressure on the pressure and temperature distribution in regard to grooved bearing, Marey [11] tested versatile speeds and loads observing the loading program of marine slow speed diesel engine. Based on wide range of conducted test trials,

the reduction of oil supply pressure under heavy loads was demonstrated to impact the maximum oil film pressure considerably. Marey et al. [12] Introduced an experimental investigation that traced the behavior of a heavy duty journal bearing in regard to slow speed diesel engines. Considering slow speed diesel engine loading program, the study examined the performance of the oil film pressure and temperature distribution profiles based on numerous variations in the most influential operational factors. Li et al. [13] investigated heavy-duty journal bearing lubrication employing elastohydrodynamic lubrication technique. Based on the conducted V8 diesel model, the dynamic characteristics of bearing are considerably affected by the structural flexibility of the shaft and bearing block. Wan et al. [14] devised a method for monitoring bearing wear from asperity contact in a diesel engine. Establishing a Thermo-Elastic Hydrodynamic Lubrication (THL) model for journal bearing on the test bench, the researchers ascertained the effectiveness of contact potential in monitoring asperity contact. Some, [15] introduced a theoretical investigation into steady-state pressure profile related to a hydrostatic double-layered porous journal bearing under turbulent regimes based on modified Reynolds equation. The load carrying capacity of the bearing under turbulent flow was demonstrated to be higher than that of laminar flow. Gu et al. [16] were focused on the effects of lubrication oil temperature and bearing structure parameters on the start-stop performance of journal bearing system. Lower lubrication oil temperature, higher final speed and lower bearing clearance were all confirmed to enhance journal bearing performance in the start-stop process. Kamat et al. [17] examined the impact of cavitation and temperature on fluid film bearing performance utilizing CFD and FSI techniques. Load carrying capacity decreased significantly with the increases in temperature due to the reduction in lubricant viscosity. Iwata et al. [18] established an innovative method to measure the oil film pressure in the main bearing of a high-speed engine during operation. Utilizing a highly durable thin-film sensor, the study stressed the importance of considering thermal deformation in simulation model construction. A numerical investigation was launched by Wang et al. [19], to analyze the performance of hydrostatic journal bearing. The study traced the impact of operating conditions and structure parameters on the maximum load capacity. The increase of eccentricity ratio was confirmed to enhance the radial load capacity. Also, the dimensionless maximum load capacity was evident to increase with the reduction in supply pressure. Apresai et al. [20] analyzed the main bearing wear in internal combustion engines. The constant supply of lubricating oil on the bearing in sufficient quantity was ascertained to reduce the bearing surface wear considerably. Bas [21] outlined the impacts of additive oil on statically loaded radial journal bearing performance. Adding inorganic compounds as additives to the engine oils utilized between shaft and bearing was assured to have a notable impact on the frictional behavior of thin-walled plain bearing. Molybdenum Disulfide

(MoS2) additives were also demonstrated to minimize wear and to extend journal bearing life. Mahdi and Abass [22] traced the impacts of lubricant compressibility and variable viscosity in regard to the static performance of three-lobe bearing via Dawson model and a computer program. Higher values of viscosity coefficient were confirmed to decrease oil film pressure and load-carrying capacity. Ahmed et al. [23] traced Thermo-Hydrodynamic (THD) behavior in finite length journal bearing lubricated with miscellaneous types of Nano-lubricants. Employing Computational Fluid Dynamic (CFD) approach, the study verified the increase of maximum pressure by 21 % in the bearing lubricated with Nano-lubricants. Kadhim et al. [24] conducted a three-dimensional CFD analysis on circular hydrodynamic journal bearing performance utilizing two different types of lubricants, SEA 10W50 and SEA 10W40. The increase in temperature was found out to decrease lubricant viscosity. Such a decrease would in turn lead to reducing bearing load carrying capacity.

Scanning previous research investigations will reveal that the effect of changing the operating conditions in medium-speed shaft journal bearing under increased loads and with different oil types on hydrodynamic lubrication has not been adequately investigated. Accordingly, the current study is basically focused on bridging the research gap by tracing the impacts of all of the three operational factors together in regard to the operational behavior of the lubricating oil film within journal bearing.

## 2. EXPERIMENTAL TEST SETUP

The Universal Journal Bearing Test Rig (UJBTR) Figure 1 is a multi-function structure that is primarily assigned with the task of investigating the critical operational factors affecting journal bearing performance. It is a grooved bearing that is provided with a number of fourteen pressure and temperature sensors distributed all around the bearing circumference Figure 2. A hydraulic power pack unit that is integrated into the discipline works on exerting versatile applied loads. The Supervisory Control and Data Acquisition (SCADA) system [9] is involved in the structure with all the essential control and monitoring devices, all of which will ensure the precision of all the tests that are to be conducted together with the related outcomes. To impose different variations regarding journal shaft speed according to the test trial requirements, a use has been made of a Variable Frequency Drive (VFD). All sensors of data logger were recalibrated; it was so crucial to carry out a number of uncertainty analyses concerning all conducted test trials as well as related outcomes. Such measurements could provide sufficient validity to the structure and could as well verify the different empirical procedures are error-free satisfactorily. Noteworthy that the test room temperature has been kept constant all through the conducted procedures. all test trials have been carried out under the same chronological and weather conditions. Also, the UJBTR structure has been run for an hour prior to each experimental test, such step was

essential to ensure realizing the steady-state condition before readings were obtained and recorded.

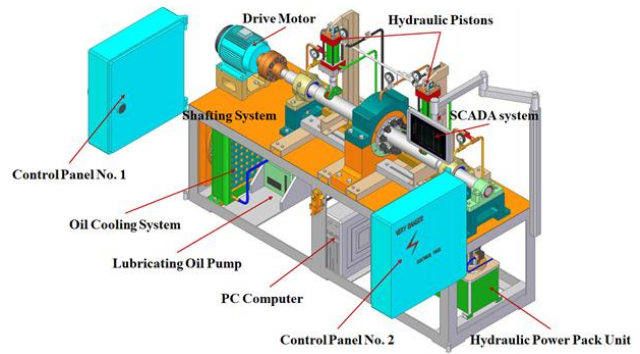


**Figure 1:** UJBTR utilized for the experimental test procedures, Marey et al. [8]

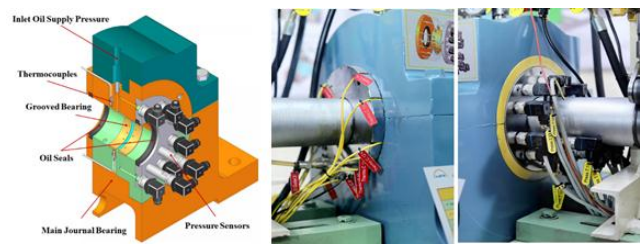


**Figure 2:** Circumferential pressure and temperature sensors on journal bearing, Marey et al. [8]

UJBTR was operated according to the operation checklist criteria, Marey et al. [8] so that the impact of different operational factors comprising speed, lubricant viscosity as well as the applied loads could each be fully traced and identified. While Table 1 includes all UJBTR specifications, Table 2 involves the technical operational data, whereas Table 3 illustrates the different oil grade properties related to the test trials. Test trial procedures can be divided into three main groups based on the type of lubricant being tested. The first of those has been focused on examining the behavior of the oil film pressure profile within journal bearing utilizing oil grade SAE 5W40 under different applied loads and at various speed ranges. Noteworthy that the second and third groups of tests have aimed at investigating the same profile previously mentioned but utilizing the different oil grades of SAE 0W30 and SAE 0W20 respectively.

**Table 1:** UJBTR specifications, Marey et al. [8]

Parameters	Value
L, Bearing Length	58 mm
D, Inner Bearing Diameter	105.05 mm
$\Phi_s$ , Shaft Diameter	104.97 mm
r, Journal Shaft Radius	52.425 mm
$C_0$ , Total Clearance	0.104 mm
C, Radial Clearance	0.052 mm
L/D, ratio	0.55

**Table 2:** Technical operational data and input parameters for test trial procedures.

Parameters	Description
Bearing Type	Circumferential Grooved Bearing
Bearing Material	White Metal
Lubricant Grade	SAE 5W40, SAE 0W30 and SAE 0W20
Inlet Oil Temperature	313 K
Operating Speeds	300, 400, 500 and 600 rpm
W, Applied Loads	50, 125, 185, 275, 470 and 510 $kg_f$

**Table 3:** Oil grade properties.

Parameters	Oil Grade Properties		
	SAE 0W20	SAE 0W30	SAE 5W40
Density at 288 K	0.841 g/ml	0.838 g/ml	0.85 g/ml
Kinematic Viscosity at 373 K	8.2 $mm^2/s$	11.8 $mm^2/s$	14 $mm^2/s$
Kinematic Viscosity at 313 K	44.8 $mm^2/s$	61 $mm^2/s$	84.7 $mm^2/s$
Viscosity Index	161	193	171
Flash Point	495 K	490 K	509 K
Pour Point	232 K	231 K	237 K

### 3. RESULTS AND DISCUSSION

The current investigation introduces a comprehensive experimental analysis regarding hydrodynamic performance utilizing UJBTR. It involves making numerous variations in the most critical operational conditions comprising oil viscosity, rotational shaft speed as well as the applied loads. Also, the impact of key operational factors on hydrodynamic lubrication and the oil film pressure distribution profile within journal bearing will be discussed. A number of results that are shown in the following figures have been derived based on testing three different oil grades (0W20, 0W30 and 5W40). The pressure values obtained under the shaft load of 50  $kg_f$ , utilizing the previously mentioned lubricant grades at different shaft speeds, were observed to be very low. Further, the maximum oil film pressure  $P_{max}$  were noted to always occur at the angle of 198°. Additionally, the value of  $P_{max}$  was evident to rise with the increase of speed and load.

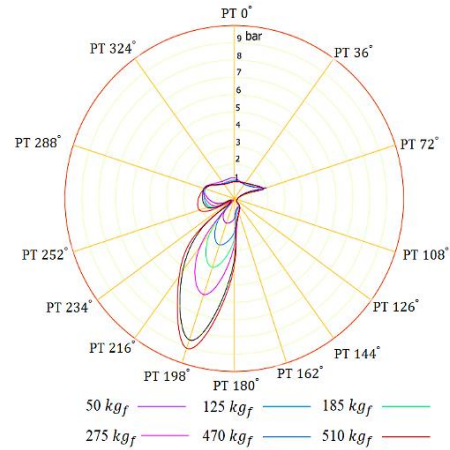


**Figure 3:** Variation of oil film pressure along the circumference of CGB (0W20, 300 rpm).

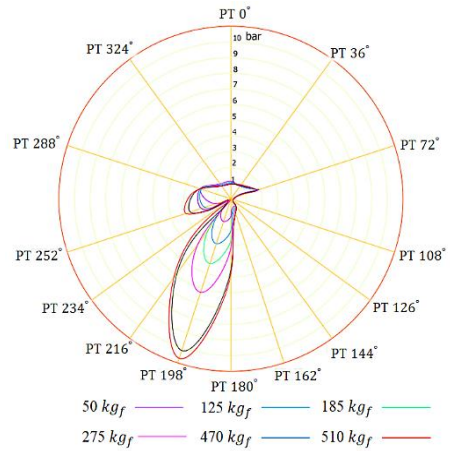


**Figure 4:** Variation of oil film pressure along the circumference of CGB (0W20, 400 rpm).

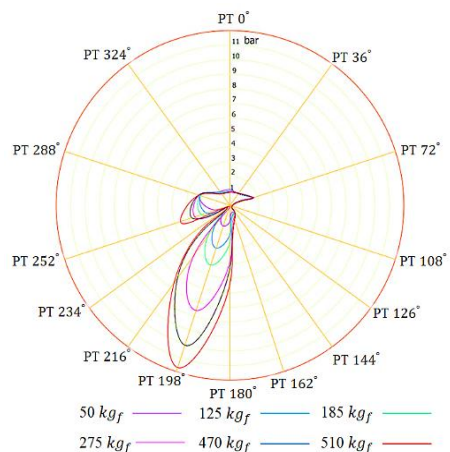


**Figure 5:** Variation of oil film pressure along the circumference of CGB (0W20, 500 rpm).

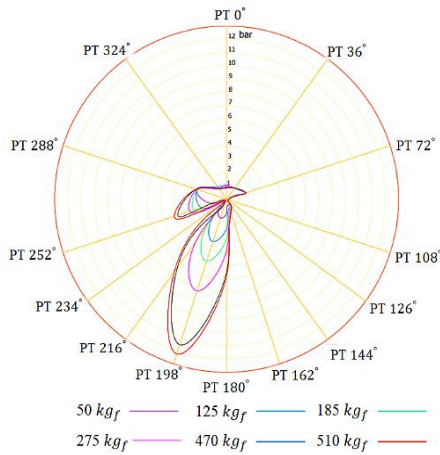


**Figure 6:** Variation of oil film pressure along the circumference of CGB (0W20, 600 rpm).

Figures (3-6) represent the recorded readings regarding the oil film pressure for 0W20 oil grade under the different loads of (50  $kg_f$ , 125  $kg_f$ , 185  $kg_f$ , 275  $kg_f$ , 470  $kg_f$ , and 510  $kg_f$ ), corresponding to the speed ranges of (300 rpm, 400 rpm, 500 rpm, and 600 rpm) respectively. Also, the increase of load for any of the aforementioned speeds incurs a rise in the  $P_{max}$  value until such value reaches its maximum when the heaviest load of 510  $kg_f$  is exerted on journal shaft. Besides, the value of  $P_{max}$  at the lowest shaft speed of 300 rpm has recorded 9.1 bar, when the highest load is exerted on rotation shaft. Further, the pressure profile features continuous increments with the increase in speed ranges, where it records the maximum value of 12.21 bar at the highest speed range of 600 rpm obtained under the heaviest applied load. That was the highest recorded value for the oil film pressure profile acquired utilizing 0W20 oil grade.

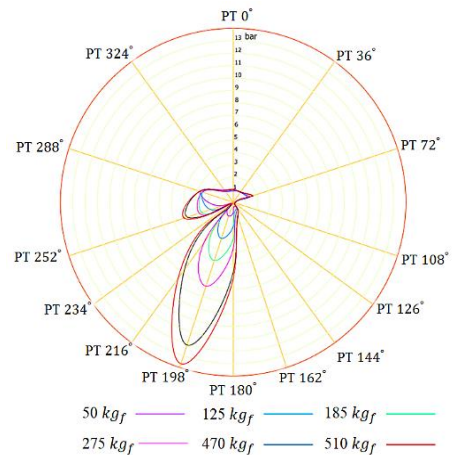


**Figure 8:** Variation of oil film pressure along the circumference of CGB (0W30, 400 rpm).

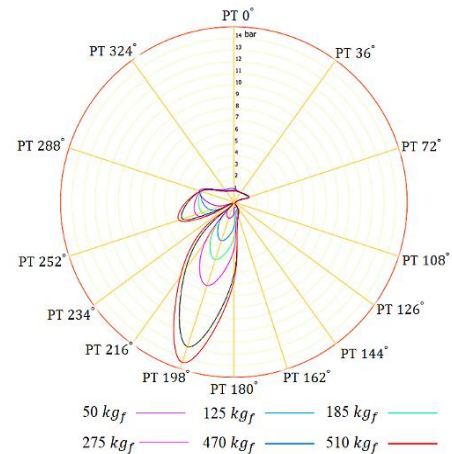


**Figure 9:** Variation of oil film pressure along the circumference of CGB (0W30, 500 rpm).

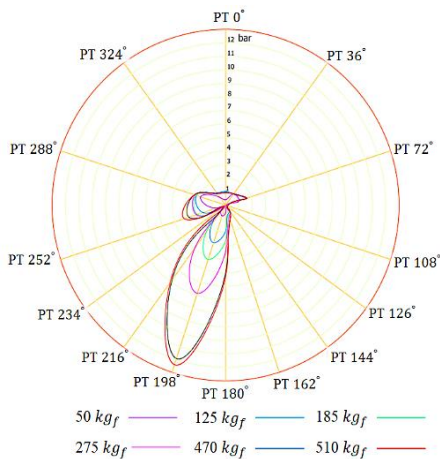


**Figure 7:** Variation of oil film pressure along the circumference of CGB (0W30, 300 rpm).

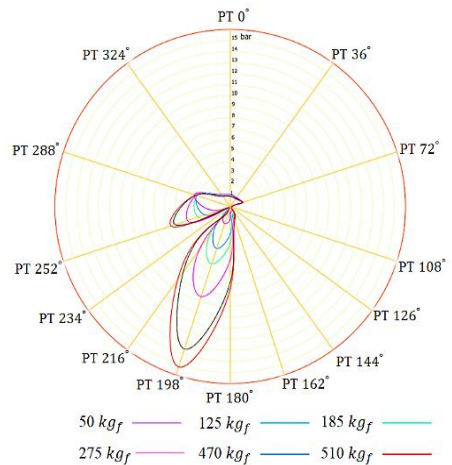


**Figure 10:** Variation of oil film pressure along the circumference of CGB (0W30, 600 rpm).

As for Figures (7-10), they illustrate the recorded readings for oil film pressure profile in regard to 0W30 oil grade. This time they were also taken at shaft speeds of (300 rpm, 400 rpm, 500 rpm and 600 rpm) for each of the

different loads involving  $50\text{ kg}_f$ ,  $125\text{ kg}_f$ ,  $185\text{ kg}_f$ ,  $275\text{ kg}_f$ ,  $470\text{ kg}_f$ , and  $510\text{ kg}_f$  consecutively. The  $P_{max}$  was found out to assume the highest value of 12.4 bar at the least shaft speed of 300 rpm and the highest exerted load of  $510\text{ kg}_f$ . Noteworthy that although such value was obtained at the least speed range, it was still higher than its highest peer value for the same profile obtained with 0W20 as clearly shown in the previous Figure (6). Additionally, the increase in the applied load at any of the experimented speed ranges incurs correspondent rises in the  $P_{max}$  value until such value assumes its maximum under the highest load of  $510\text{ kg}_f$ . Also, pressure values tend to increase with the increments in speed ranges until  $P_{max}$  reaches the maximum value of 15.23 bar at the highest speed of 600 rpm under the heaviest load. Thus, the highest recorded value for oil film pressure profile was evidently obtained utilizing 0W30 oil grade.

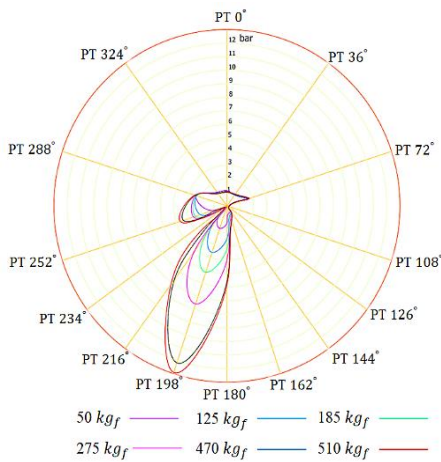


**Figure 11:** Variation of oil film pressure along the circumference of CGB (5W40, 300 rpm).

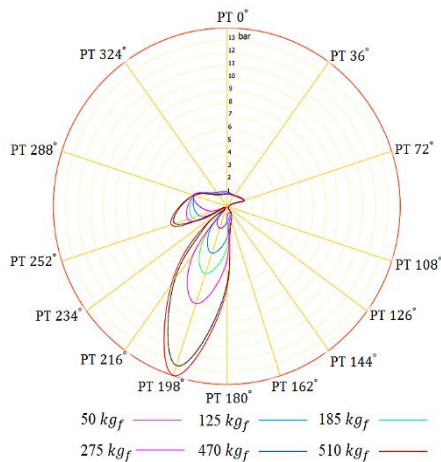


**Figure 12:** Variation of oil film pressure along the circumference of CGB (5W40, 400 rpm).

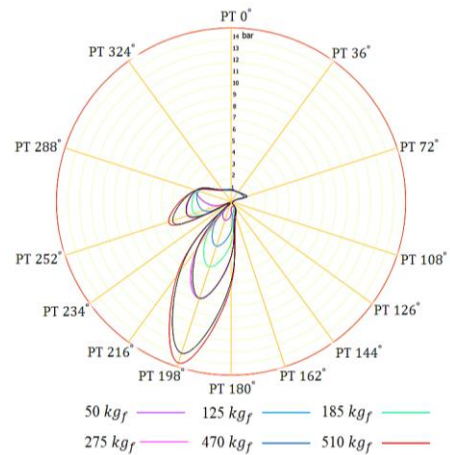


**Figure 13:** Variation of oil film pressure along the circumference of CGB (5W40, 500 rpm).

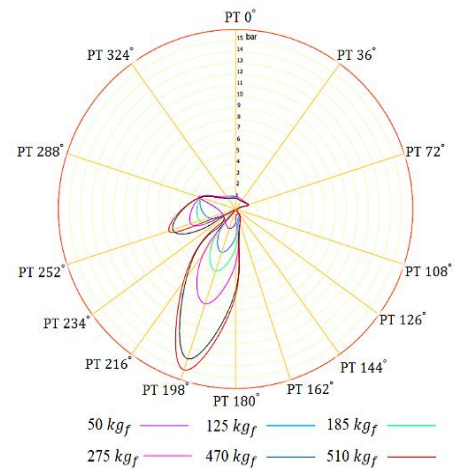


**Figure 14:** Variation of oil film pressure along the circumference of CGB (5W40, 600 rpm).

Figures (11-14) point out the obtained readings for oil film pressure profile with 5W40 lubricant grade. Again, those were recorded under the same speed and load operating conditions mentioned before. Here, the  $P_{max}$  has assumed the highest value of 12.91 bar at the least speed range of 300 rpm and under the highest load of  $510\text{ kg}_f$ . It is noted that the  $P_{max}$  value has slightly increased by 0.5 bar compared to 0W30 oil grade at the same speed and load conditions as clearly shown in Figure 7. Pressure increases with the buildup of speed and load until  $P_{max}$  reaches a peak of 15.07 bar at the highest speed of 600 rpm and under the heaviest load. This is obviously the highest value assumed by the oil film pressure profile and it was obtained with 5W40 oil grade.

#### 4. THEORETICAL INVESTIGATION

For investigation purposes, a theoretical analysis has been conducted for checking and better identifying the accuracy of the results derived experimentally utilizing the theoretical bearing characteristic number analysis

(Sommerfeld number, S), [25]. It involved testing the three lubricant grades under study at the speed range of 300 rpm under the variable applied lateral loads from 50 kg up to 510 kg. Further, to ascertain UJBTR results validity, the following procedures were carried out. Bearing characteristic number (Sommerfeld number, S) was calculated utilizing equations (1) and (2).

$$S = \left(\frac{r}{c}\right)^2 \frac{\mu N}{P} \dots\dots\dots (1)$$

Where (P) is the pressure on the projected area

$$P = W/2rl \dots\dots\dots (2)$$

Using the Chart of determining the maximum film pressure ratio [25], with  $(l/d) = 0.5$  ratio and (S), the theoretical values of the maximum film pressure ratio ( $P_0/P_{max}$ ) are reproduced below in Table (4-6).

**Table 4:** Experimental results Vs Theoretical results (0W20 at 300 rpm).

Load	Theoretical ( $P_0/P_{max}$ )	Experimental ( $P_0/P_{max}$ )	Deviation ( $P_0/P_{max}$ )	Error %
50 kg <sub>f</sub>	0.51	0.53	-0.02	3.9 %
125 kg <sub>f</sub>	0.46	0.48	-0.02	4.3 %
185 kg <sub>f</sub>	0.42	0.4	0.02	4.8 %
275 kg <sub>f</sub>	0.41	0.39	0.02	4.9 %
470 kg <sub>f</sub>	0.36	0.35	0.01	2.8 %
510 kg <sub>f</sub>	0.35	0.33	0.02	5.7 %

**Table 5:** Experimental results Vs Theoretical results (0W30 at 300 rpm).

Load	Theoretical ( $P_0/P_{max}$ )	Experimental ( $P_0/P_{max}$ )	Deviation ( $P_0/P_{max}$ )	Error %
50 kg <sub>f</sub>	0.52	0.55	-0.03	5.8 %
125 kg <sub>f</sub>	0.481	0.5	-0.019	4.0 %
185 kg <sub>f</sub>	0.46	0.47	-0.01	2.2 %
275 kg <sub>f</sub>	0.42	0.41	0.01	2.4 %
470 kg <sub>f</sub>	0.38	0.37	0.01	2.6 %
510 kg <sub>f</sub>	0.37	0.36	0.01	2.7 %

**Table 6:** Experimental results Vs Theoretical results (5W40 at 300 rpm).

Load	Theoretical ( $P_0/P_{max}$ )	Experimental ( $P_0/P_{max}$ )	Deviation ( $P_0/P_{max}$ )	Error %
50 kg <sub>f</sub>	0.522	0.54	-0.018	3.4 %
125 kg <sub>f</sub>	0.5	0.51	-0.01	2.0 %
185 kg <sub>f</sub>	0.48	0.48	0.0	0 %
275 kg <sub>f</sub>	0.445	0.42	0.025	5.6 %
470 kg <sub>f</sub>	0.41	0.387	0.023	5.6 %
510 kg <sub>f</sub>	0.405	0.381	0.024	5.9 %

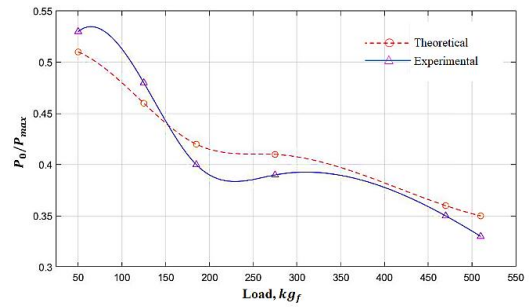


**Figure 15:** Outlines the variation values as observed between the experimental and theoretical results for 0W20 Oil at 300 rpm.

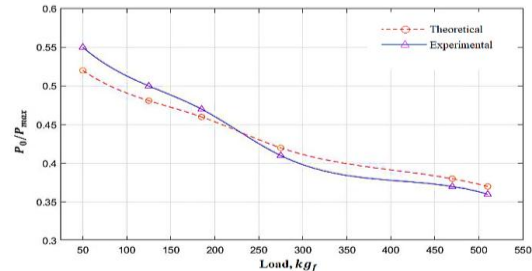


**Figure 16:** Outlines the variation values as observed between the experimental and theoretical results for 0W30 Oil at 300 rpm

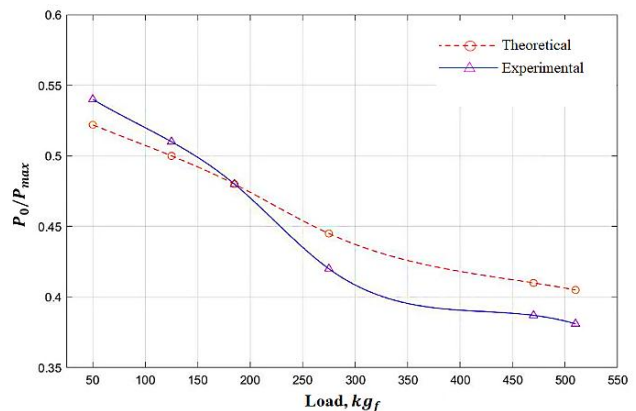


**Figure 17:** Outlines the variation values as observed between the experimental and theoretical results for 5W40 Oil at 300 rpm

The validation criteria involve the Maximum film pressure ratio " $P_0/P_{max}$ ", where  $P_0$  represents the terminating oil film pressure and  $P_{max}$  symbolizes the maximum oil film pressure. Tables (4-6) show the measured and the derived  $P_0/P_{max}$  values. Figures (15-17) reveal that the obtained deviation is within the acceptable limits. The maximum error percentage was marginal and it was 5.9 %, an outcome which adds to the previously referred to uncertainty analyses sufficient validation regarding the experimental results.

The primary focus of the study at hand was to introduce the effect of mixing different operational parameters over journal bearing pressure profiles. Additionally, it is intended to outline the full impact of all the above-mentioned operational factors on the hydrodynamic

lubrication which is outlined by the values of the coefficient of friction ( $f$ ) and characteristic number ( $Z$ ). Furthermore, the study scope is concerned with the speed ranges of (300 rpm, 400 rpm, 500 rpm and 600 rpm) and is also basically confined to certain loads comprising (50  $kg_f$ , 125  $kg_f$ , 185  $kg_f$  and 275  $kg_f$ ) respectively. In addition, the viscosities related to the three oil grades involved in the experimental test trials are (44.8 mm<sup>2</sup>/s, 61 mm<sup>2</sup>/s and 84.7 mm<sup>2</sup>/s). The coefficient of friction and characteristic number values were also calculated as outlined in Tables (7-10). Those values are instrumental in identifying the friction values between interlayers of oil film. That in turn will explain and will also account for the power loss during hydrodynamic lubrication. Also, the value of the characteristic number will reflect how far or close lubrication is likely to turn from the hydrodynamic lubrication to the transient or boundary lubrication one occurring at the value of ( $1.7 * 10^{-6}$ ) [25].

$$Z = \frac{\mu N}{P} \dots\dots\dots(3)$$

$$f = 2\pi^2 \frac{\mu N}{P} \frac{r}{c} \dots\dots\dots(4)$$

**Table 7: Load = 50  $kg_f$ .**

Type of oil	N (rpm)	$\mu$ (Pa.s)	$f$	P (pas)	Z	S
0W20	300	0.03696	4.74E-02	80657	2.29E-06	2.52
	400	0.03687	6.30E-02	80657	3.05E-06	3.35
	500	0.03683	7.87E-02	80657	3.80E-06	4.18
	600	0.03679	9.43E-02	80657	4.56E-06	5.01
0W30	300	0.05002	6.41E-02	80657	3.10E-06	3.41
	400	0.04986	8.52E-02	80657	4.12E-06	4.53
	500	0.04974	1.06E-01	80657	5.14E-06	5.65
	600	0.04974	1.28E-01	80657	6.17E-06	6.78
5W40	300	0.07051	9.04E-02	80657	4.37E-06	4.81
	400	0.07035	1.20E-01	80657	5.81E-06	6.39
	500	0.07023	1.50E-01	80657	7.26E-06	7.98
	600	0.07014	1.80E-01	80657	8.70E-06	9.56

**Table 8: Load = 125  $kg_f$ .**

Type of oil	N (rpm)	$\mu$ (Pa.s)	$f$	P (pas)	Z	S
0W20	300	0.03692	1.89E-02	201643	9.15E-07	1.01
	400	0.03687	2.52E-02	201643	1.22E-06	1.34
	500	0.03683	3.15E-02	201643	1.52E-06	1.67
	600	0.03679	3.77E-02	201643	1.82E-06	2.01
0W30	300	0.04997	2.56E-02	201643	1.24E-06	1.36
	400	0.04986	3.41E-02	201643	1.65E-06	1.81
	500	0.04974	4.25E-02	201643	2.06E-06	2.26
	600	0.04972	5.10E-02	201643	2.47E-06	2.71
5W40	300	0.07047	3.61E-02	201643	1.75E-06	1.92
	400	0.07035	4.81E-02	201643	2.33E-06	2.56
	500	0.07020	6.00E-02	201643	2.90E-06	3.19
	600	0.07010	7.19E-02	201643	3.48E-06	3.82

**Table 9: Load = 185  $kg_f$ .**

Type of oil	N (rpm)	$\mu$ (Pa.s)	$f$	P (pas)	Z	S
0W20	300	0.03690	1.28E-02	298431	6.18E-07	0.68
	400	0.03686	1.70E-02	298431	8.23E-07	0.91
	500	0.03682	2.13E-02	298431	1.03E-06	1.13
	600	0.03677	2.55E-02	298431	1.23E-06	1.35
0W30	300	0.04997	1.73E-02	298431	8.37E-07	0.92
	400	0.04982	2.30E-02	298431	1.11E-06	1.22
	500	0.04974	2.87E-02	298431	1.39E-06	1.53
	600	0.04972	3.44E-02	298431	1.67E-06	1.83
5W40	300	0.07045	2.44E-02	298431	1.18E-06	1.30
	400	0.07029	3.25E-02	298431	1.57E-06	1.73
	500	0.07018	4.05E-02	298431	1.96E-06	2.15
	600	0.07008	4.86E-02	298431	2.35E-06	2.58

**Table 10: Load = 185  $kg_f$ .**

Type of oil	N (rpm)	$\mu$ (Pa.s)	$f$	P (pas)	Z	S
0W20	300	0.03689	8.60E-03	443614	4.16E-07	0.46
	400	0.03686	1.15E-02	443614	5.54E-07	0.61
	500	0.03682	1.43E-02	443614	6.92E-07	0.76
	600	0.03676	1.71E-02	443614	8.29E-07	0.91
0W30	300	0.04994	1.16E-02	443614	5.63E-07	0.62
	400	0.04979	1.55E-02	443614	7.48E-07	0.82
	500	0.04973	1.93E-02	443614	9.34E-07	1.03
	600	0.04970	2.32E-02	443614	1.12E-06	1.23
5W40	300	0.07041	1.64E-02	443614	7.94E-07	0.87
	400	0.07024	2.18E-02	443614	1.06E-06	1.16
	500	0.07016	2.72E-02	443614	1.32E-06	1.45
	600	0.07006	3.27E-02	443614	1.58E-06	1.74

A dimensionless analysis has been conducted regarding the determined operational factors of speed, viscosities and loads and their impact on the coefficient of friction and the characteristic number via three scenarios‘

- The first scenario involves keeping load and viscosity constant at their lowest values while making degrading speed variations as shown in Table 11.
- The second scenario involves keeping load and speed constant at their lowest values with degrading variations in viscosity as outlined in Table 12.
- The third scenario involves keeping speed and viscosity constant at the least values while changing and increasing load as represented by Table 13.

**Table 11: Load = 50  $kg_f$ , 0W20 oil, and different speeds.**

Speed	Speed %	$f$	$f$ %	Z
600 rpm	100 %	0.094	100 %	$4.56 * 10^{-6}$
500 rpm	67 %	0.078	67 %	$3.80 * 10^{-6}$
400 rpm	33 %	0.063	33 %	$3.05 * 10^{-6}$
300 rpm	0 %	0.047	0 %	$2.29 * 10^{-6}$

**Table 12: Load = 50  $kg_f$ , Speed = 300 rpm, and different Viscosities.**

Viscosity (m <sup>2</sup> /s)	Viscosity %	$f$	$f$ %	Z
$8.47 * 10^{-5}$	100 %	0.090	100 %	$4.37 * 10^{-6}$
$6.10 * 10^{-5}$	41 %	0.064	39 %	$3.10 * 10^{-6}$
$4.48 * 10^{-5}$	0 %	0.047	0 %	$2.29 * 10^{-6}$

**Table 13:** Speed = 300 rpm, 0W20 oil, and different Loads.

Load	Load %	$f$	$f$ %	$Z$
50 $kg_f$	0 %	0.047	100 %	$2.29 * 10^{-6}$
125 $kg_f$	33 %	0.018	27 %	$9.15 * 10^{-7}$
185 $kg_f$	60 %	0.012	11 %	$6.18 * 10^{-7}$
275 $kg_f$	100 %	0.008	0 %	$4.16 * 10^{-7}$

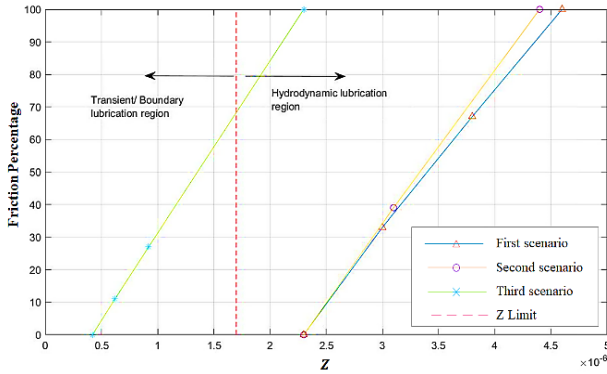


**Figure 18:** Coefficient of friction Vs Characteristic number.

From the previous curve shown in Figure 18, the slope of the curve of the third scenario was more than those involved in the first and second scenarios. Such an outcome indicates that the load factor exerts a greater impact on both friction and hydrodynamic lubrication. Further, it is observed in the first and second scenarios that all characteristic number values are higher than ( $1.7 * 10^{-6}$ ). The fact that refers to hydrodynamic lubrication. Also, the value derived based on the third scenario was higher than ( $1.7 * 10^{-6}$ ) only when the applied load is 50  $kg_f$ . However, for the heavier loads of 125  $kg_f$ , 185  $kg_f$  and 275  $kg_f$ , the values of the characteristic number were less than ( $1.7 * 10^{-6}$ ), indicating the transition of lubrication to the transient or boundary lubrication.

Considering the positive relation between speed and viscosity on one side and the coefficient of friction and the characteristic number on the other, the impact of reducing speed by 60 % on the friction between oil films and hydrodynamic lubrication boundaries was investigated. Moreover, the study scope has extended to cover the impact of reducing viscosity by 60 % regarding the same research domains. Based on the negative relation between load and both the coefficient of friction and the characteristic number, the impact of increasing load by 60 % on the friction between oil films and hydrodynamic lubrication was investigated (Table 14).

**Table 14:** similarity analysis.

Decreasing the Speed by 60%				
Speed	Speed %	$f$	$f$ %	$Z$
420 rpm	40 %	$6.61 * 10^{-2}$	40 %	$3.20 * 10^{-6}$
Decreasing the Viscosity by 60%				
Viscosity	Viscosity %	$f$	$f$ %	$Z$
$6.06 * 10^{-5}$ m <sup>2</sup> /s	40 %	$6.37 * 10^{-2}$	38 %	$3.08 * 10^{-6}$
Increasing the Load by 60%				
Load	Load %	$f$	$f$ %	$Z$
185 $kg_f$	60 %	$1.28 * 10^{-2}$	11 %	$6.18 * 10^{-7}$

In light of the previous Table 14, it is observed that the decrease of speed by 60 % has led to a similar decrease of friction coefficient also by 60 %. Further, the decrease of viscosity by 60 % has had a little greater impact on the coefficient of friction leading it to decrease by 62 %. As for the impact of increasing load by 60 %, it was found to reduce the coefficient of friction considerably by a percentage of 89 %. Regarding the hydrodynamic lubrication limits, the reduction of viscosity by 60 % was concluded to have a little greater negative impact on the hydrodynamic lubrication compared to that recorded when speed is reduced by the same percentage of 60 %. Additionally, the increase of load by 60 % has been ascertained to have a very serious and negative impact on hydrodynamic lubrication, and the lubrication has turned from hydrodynamic lubrication to transient or boundary lubrication as outlined by the previous table.

## 5. CONCLUSIONS

Based on the derived outcomes, maximum oil film pressure increases with load and speed increments at constant viscosity and variable increasing loads from 50  $kg_f$  up to 510  $kg_f$ . Higher viscosity oil grades incur a higher rise in  $P_{max}$  value. It is thus concluded that the increased applied loads decrease the relative motion between the interlayers of oil film and hence the outcome pressure gets higher. However, increased load has a negative impact mainly represented in power loss due to the maximized friction between oil interlayers. Also, at specific speed ranges with lower viscosity lubricants, the characteristic number decreases. A clear indication of transition into the transient or boundary lubrication region. It is under such operating conditions that the produced pressure will be insufficient for shaft weight and thus the metal-to-metal contact appears. For elaborate discussions, a dimensionless analysis was conducted to identify how far the characteristic number ( $Z$ ) and the friction coefficient ( $f$ ) are affected by variations made in viscosity, speed and load factors. The coefficient of friction decreases by 60 % on reducing speed range by the same percentage. In comparison, decreasing viscosity by 60 % incurs a significant impact on friction Coefficient amounting to 62 %. Thus, the decrease of viscosity by 60 % is evident to have a little more impact on hydrodynamic lubrication boundaries, compared to that obtained at speed reduction with the same percentage. Yet, the increase of load by 60

% affects hydrodynamic lubrication negatively. It is under such conditions that transient or boundary lubrication shows signs. Hence, it is recommended to adjust shaft weights according to speed and viscosity criteria at the initial phases of journal bearing design. In such a way, transient lubrication boundaries could be avoided and friction losses could be reduced simultaneously.

### Nomenclature

$C_o$	Total clearance	mm
$C$	Radial clearance	mm
$D$	Inner diameter for grooved bearing	mm
$L$	Bearing length	mm
$N$	Shaft speed	rpm
$P_0$	Terminating oil film pressure	bar
$P_{max}$	Maximum oil film pressure	bar
$\Phi_s$	Shaft diameter	mm
$r$	Radius for Journal Shaft	mm
$T$	Temperature	K

### Dimensionless Group

$P_0/P_{max}$	maximum film pressure ratio
$L/D$	Bearing length/inner diameter
$Z$	Bearing characteristic number

### Greek Letters

$\mu$	Dynamic oil viscosity	Pa.s
$f$	Coefficient of friction	

### Abbreviations

PT	Pressure transmitter
SCADA	Supervisory control and data acquisition
TC	Thermocouple
UJBTR	Universal Journal Bearing Test Rig
VFD	Variable frequency drive

### Credit Authorship Contribution Statement:

**Nader Nasr:** Methodology, Conceptualization, Writing, Visualization, Resources and Original draft.

**Ahmed. Abdelsalam, Amman. A. Ali and Nour. A. Marey:** Writing, Reviewing and Editing

### Declaration of Competing Interest

The authors declare that they have no known competing financial interests or personal relationships that could have appeared to influence the work reported in this paper.

## 6. REFERENCES

[1] K. G. Binu, K. Yathish, R. Mallya, B. S. Shenoy, D. S. Rao, and R. Pai, 'Experimental study of

hydrodynamic pressure distribution in oil lubricated two-axial groove journal bearing', *Mater. Today Proc.*, vol. 2, no. 4–5, pp. 3453–3462, 2015, doi: 10.1016/j.matpr.2015.07.321.

[2] N. M. Joy and L. Roy, 'Determination of optimum configuration among different configurations of two-axial groove hydrodynamic bearings', *Proc. Inst. Mech. Eng. Part J J. Eng. Tribol.*, vol. 230, no. 9, pp. 1071–1091, Sep. 2016, doi: 10.1177/1350650115625604.

[3] S. Chatterton, P. V. Dang, P. Pennacchi, A. De Luca, and F. Flumian, 'Experimental evidence of a two-axial groove hydrodynamic journal bearing under severe operation conditions', *Tribol. Int.*, vol. 109, pp. 416–427, 2017, doi: 10.1016/j.triboint.2017.01.014.

[4] Y. Zhang, X. Li, C. Dang, D. Hei, X. Wang, and Y. Lü, 'A semianalytical approach to nonlinear fluid film forces of a hydrodynamic journal bearing with two axial grooves', *Appl. Math. Model.*, vol. 65, pp. 318–332, Jan. 2019, doi: 10.1016/j.apm.2018.07.048.

[5] B. Roy and S. Dey, 'Machine learning-based performance analysis of two-axial-groove hydrodynamic journal bearings', *Proc. Inst. Mech. Eng. Part J J. Eng. Tribol.*, vol. 235, no. 10, pp. 2211–2224, Oct. 2021, doi: 10.1177/1350650121992895.

[6] N. Marey, E.-S. Hegazy, and A. Aly, 'Design and Setup for a Journal Bearing Universal Test Rig', *Port-Said Eng. Res. J.*, vol. 22, no. 1, pp. 101–106, Mar. 2018, doi: 10.21608/pserj.2018.32472.

[7] N. Marey, 'An Experimental Investigation of Hydrodynamic Journal Bearing with Different Oil Grades', *Port-Said Eng. Res. J.*, vol. 23, no. 2, pp. 46–54, Sep. 2019, doi: 10.21608/pserj.2019.49576.

[8] N. Marey, E.-S. Hegazy, H. El-Gamal, A. Ali, and R. Abd-El-Ghany, 'Development of A Universal Journal Bearing Test Rig (UJBTR) and Experimental Setup for Oil Film Lubrication Enhancement Regarding Marine Applications.', *Port-Said Eng. Res. J.*, no. 2, pp. 0–0, 2021, doi: 10.21608/pserj.2021.100583.1149.

[9] N. A. Marey and A. A. Ali, 'Novel measurement and control system of universal journal bearing test rig for marine applications', *Alexandria Engineering Journal*, vol. 73. Elsevier B.V., pp. 11–26, Jul. 15, 2023. doi: 10.1016/j.aej.2023.04.006.

[10] N. A. Marey, E.-S. Hegazy, H. El-Gamal, A. Ali, and R. Ramadan, 'Universal journal bearing test rig uncertainty and validation measurement to enhance marine shafting performance', *Int. Marit. Transp. Logist. J.*, vol. 11, no. 0, p. 39, 2022, doi: 10.21622/marlog.2022.11.039.

[11] N. Marey, 'Experimental Evaluation of the Effect of Oil Supply Pressure related to Marine Slow Speed Diesel Engine on Oil Film Pressure and Temperature Profiles within Journal Bearing',

- Port-Said Eng. Res. J.*, vol. 0, no. 0, pp. 0–0, 2023, doi: 10.21608/pserj.2023.194191.1221.
- [12] N. A. Marey, W. M. El- Maghlany, and M. Fayed, ‘Experimental study on hydro- thermal behavior of journal bearing oil film profile in a slow speed diesel engine’, *Alexandria Eng. J.*, vol. 81, no. October, pp. 532–547, 2023, doi: 10.1016/j.aej.2023.09.049.
- [13] W. Li, J. Liu, L. Chen, Z. Liu, and B. Zhuang, ‘Study on heavy-duty journal bearing lubrication based on Elasto-hydrodynamic lubrication method’, in *Journal of Physics: Conference Series*, Institute of Physics Publishing, Nov. 2019. doi: 10.1088/1742-6596/1314/1/012117.
- [14] B. Wan, J. Yang, and S. Sun, ‘A method for monitoring lubrication conditions of journal bearings in a diesel engine based on contact potential’, *Appl. Sci.*, vol. 10, no. 15, Aug. 2020, doi: 10.3390/app10155199.
- [15] S. Some, ‘Analysis of the steady-state pressure profile of a double-layered porous journal bearing under turbulent regimes’, *Proc. Inst. Mech. Eng. Part E J. Process Mech. Eng.*, 2022, doi: 10.1177/09544089221144397.
- [16] C. Gu, L. Dai, and D. Zhang, ‘Research on Start-Stop Performance of Journal Bearing Based on an Isothermal and Mixed Lubrication Model With Different Acceleration and Deceleration Forms in Consideration’, *J. Tribol.*, vol. 145, no. 5, May 2023, doi: 10.1115/1.4056517.
- [17] H. Kamat, C. R. Kini, and S. B. Shenoy, ‘Effect of Cavitation and Temperature on Fluid Film Bearing Using CFD and FSI Technique: A Review’, *Archives of Computational Methods in Engineering*, vol. 30, no. 3. Springer Science and Business Media B.V., pp. 1623–1636, Apr. 01, 2023. doi: 10.1007/s11831-022-09847-z.
- [18] T. Iwata *et al.*, ‘The Verification of Engine Analysis Model Accuracy by Measuring Oil Film Pressure in the Main Bearings of a Motorcycle High-Speed Engine Using a Thin-Film Sensor’, *Lubricants*, vol. 10, no. 11, Nov. 2022, doi: 10.3390/lubricants10110314.
- [19] J. Wang, J. Huang, S. Jiang, A. N. Kouediatouka, Q. Liu, and G. Dong, ‘Analysis of maximum radial load capacity of hydrostatic journal bearing considering supply pressure limitation by a novel method’, *Tribol. Int.*, vol. 184, Jun. 2023, doi: 10.1016/j.triboint.2023.108484.
- [20] E. P. Apresai, E. P. Apresai, T. A. Kilakime, and E. A. Ogbonnaya, ‘Main Bearing Wear Analysis At Varying Load And Speed Of The Engine’, *www.irjmets.com @International Res. J. Mod. Eng.*, vol. 497, 2022, [Online]. Available: www.irjmets.com
- [21] H. Baş, ‘Tribological properties of MoS<sub>2</sub> particles as lubricant additive on the performance of statically loaded radial journal bearings’, *Turkish J. Eng.*, vol. 7, no. 1, pp. 42–48, 2023, doi: 10.31127/tuje.1016153.
- [22] M. A. Mahdi and B. A. Abass, ‘Effect of lubricant compressibility and variable viscosity on the performance of three-lobe journal bearing’, *Arch. Mech. Eng.*, vol. 69, no. 2, pp. 203–219, 2022, doi: 10.24425/ame.2022.140412.
- [23] S. Y. Ahmed, B. A. Abass, and Z. H. Kadhim, ‘Cfd Analysis Of Thermohydrodynamic Behavior Of Nanolubricated Journal Bearings Considering Cavitation Effect’, *J. Serbian Soc. Comput. Mech.*, vol. 15, no. 1, pp. 110–130, 2021, doi: 10.24874/jsscm.2021.15.01.08.
- [24] Z. H. Kadhim, L. Hammed, F. A. Rahima, and A. M. Ridha, ‘Elastohydrodynamic Analysis Of A Journal Bearing With Different Grade Oils Considering Thermal And Cavitation Effects Using Cfd-Fsi’, *Diagnostyka*, vol. 24, no. 2, 2023, doi: 10.29354/diag/166102.
- [25] Shigley, C. R. Mischke, and R. G. Budynas, *Mechanical Engineering Design*, Tenth Edit. 2002.